Journal of Materials Chemistry B

ROYAL SOCIETY OF CHEMISTRY

PAPER

View Article Online
View Journal | View Issue

Published on 05 March 2025. Downloaded by CHANG GUNG UNIVERSITY on 3/26/2025 1:38:55 PM.

Check for updates

Cite this: *J. Mater. Chem. B*, 2025, **13**, 4225

Surface moieties drive the superior protection of curcumin-derived carbon quantum dots against retinal ischemia-reperfusion injury†

Ming-Hui Sun,[ab] Kuan-Jen Chen,[ab] Yu-Ting Tsao,[a] Chi-Chin Sun,[ac] Jui-Yang Lai,[adef] Chin-Jung Lin,[g] Yu-Fen Huang[g] and Chih-Ching Huang*[hij]

Received 21st October 2024,
Accepted 2nd March 2025

DOI: 10.1039/d4tb02364a

rsc.li/materials-b

Despite the recognized neuroprotective benefits of curcumin, its clinical utility is constrained by poor bioavailability and high cytotoxicity at effective doses. This study evaluates the therapeutic potential of curcumin-derived carbon quantum dots (Cur-CQDs) for retinal protection against ischemia-reperfusion (IR) injury in rats. Cur-CQDs were synthesized *via* mild pyrolysis at varying temperatures and assessed for efficacy in rat retinal ganglion cells and a model of retinal IR injury. The Cur-CQDs, particularly those synthesized at 150 °C, displayed significant reductions in apoptosis in retinal tissues, as indicated by TUNEL assays, immunofluorescence localization of HIF-α, CD68, BCL-2, and Grp78, and Western blot analysis for HO-1, Grp78, CHOP, caspase 3, and Nrf2. These results suggest that Cur-CQDs not only enhance cell survival and reduce inflammation but also decrease oxidative and endoplasmic reticulum stress markers. Mechanistic insights reveal that Cur-CQDs modulate pathways involved in oxidative stress, apoptosis, and inflammation, specifically through the upregulation of BCL-2 and HO-1 and the downregulation of CHOP, caspase-3, and endoplasmic reticulum stress markers. The identification of cinnamic acid-, anisole-, guaiacol, and ferulic acid-like structures on Cur-CQDs' surfaces may contribute to their superior antioxidative and anti-inflammatory activities. Collectively, these findings position Cur-CQDs as a promising approach for treating retinal IR injuries, enhancing curcumin's bioavailability and therapeutic efficacy, and paving new pathways in ocular neuroprotection research and potential clinical applications.

Introduction

Curcumin (1,7-bis-(4-hydroxy-3-methoxyphenyl)-1,6-heptadiene-3,5-dione) is a natural polyphenol product extracted from turmeric (Curcuma longa) that has long been advocated for the treatment of a variety of conditions including neurodegenerative and inflammatory disorders.[1,2] In animal models, it has been demonstrated to have beneficial effects on rodent models of cancer, diabetes, cardiovascular diseases, arthritis and Alzheimer's disease.[1–3] In ocular tissue, curcumin also has been shown to possess neuronal and vascular protection against retinal ischemia-reperfusion (IR) injury in a rat model through the reduction of inflammatory cytokines, attenuation of mitochondrial-mediated oxidative stress, and amelioration of inflammatory responses *via* PPAR-γ agonist activity.[4–9] Intragastric administration of curcumin (10 mg kg^{-1} per day) (equal to a human dosage of 800 mg per day) in a rodent model of ocular hypertension was reported to have protection from retinal microglial death.[10] However, increased systemic side effects from higher or repeated dosages of curcumin along with curcumin's poor water solubility and low bioavailability

[a] *Department of Ophthalmology, Chang Gung Memorial Hospital, Linkou, Taoyuan, 33305, Taiwan*
[b] *College of Medicine, Chang Gung University, Taoyuan 33302, Taiwan*
[c] *Department of Ophthalmology, Chang Gung Memorial Hospital, Keelung, 20401, Taiwan*
[d] *Department of Biomedical Engineering, Chang Gung University, Taoyuan 33302, Taiwan*
[e] *Department of Materials Engineering, Ming Chi University of Technology, New Taipei City, 24301, Taiwan*
[f] *Research Center for Chinese Herbal Medicine, College of Human Ecology, Chang Gung University of Science and Technology, Taoyuan, 33303, Taiwan*
[g] *Institute of Analytical and Environmental Sciences, National Tsing Hua University, Hsinchu, 30013, Taiwan*
[h] *Department of Bioscience and Biotechnology, National Taiwan Ocean University, Keelung, 20224, Taiwan. E-mail: huanging@ntou.edu.tw*
[i] *Center of Excellence for the Oceans, National Taiwan Ocean University, Keelung 20224, Taiwan*
[j] *School of Pharmacy, College of Pharmacy, Kaohsiung Medical University, Kaohsiung 80708, Taiwan*

† Electronic supplementary information (ESI) available: The details on the chemicals, experimental methods, and Fig. S1–S7. See DOI: https://doi.org/10.1039/d4tb02364a

Published on 05 March 2025. Downloaded by CHANG GUNG UNIVERSITY on 3/26/2025 1:38:55 PM.

contribute to its limitation of clinical use.[3,11,12] Topical curcumin-loaded nanoparticles have been developed for sustained release to improve the effectiveness of the drug, and have been shown to reduce retinal ganglion cells (RGCs) loss in a rodent model of optic nerve disease and ocular hypertension.[13] However, the cytotoxicity and biocompatibility of nanoparticles have raised serious concerns about their impact on human health and the environment.[14,15]

The emergence of carbon dots (CDs), including graphene quantum dots (GQDs), carbon quantum dots (CQDs), and carbonized polymer dots (CPDs), has opened new avenues in the development of nanotherapeutics aimed at treating inflammatory diseases.[16–22] These CDs are synthesized through carbonization processes where organic precursors are thermally decomposed or chemically transformed into carbonaceous nanoparticles. This synthesis process imbues the CDs with unique properties such as high surface area, tunable particle sizes, and the capacity for surface functionalization, making them ideal candidates for biomedical applications. These antioxidative CDs exhibit a remarkable ability to scavenge reactive oxygen species (ROS), reducing oxidative stress, a critical factor in the pathogenesis of various inflammatory conditions.[23–26] Moreover, they have been shown to modulate key inflammatory pathways, including NF-κB and MAPK signaling, thereby exerting potent anti-inflammatory effects.[27] This multi-functionality not only highlights their therapeutic potential but also offers a multifaceted approach to managing inflammation, potentially leading to treatments that are both more effective and specific. A recent study has shown that CDs can significantly reduce inflammation in models of arthritis, suggesting their potential as a novel therapeutic strategy for rheumatoid arthritis.[28] Similarly, CQDs have been explored for their therapeutic effects in models of neuroinflammatory diseases, where they have been found to attenuate symptoms and modulate inflammatory responses.[29–33] These findings underscore the versatility and promise of carbonized nanomaterials in the context of inflammatory disease treatment, paving the way for the development of new nanotherapeutics that could revolutionize the management of inflammation-related conditions. However, the impact of intact moiety structures on the carbonized nanomaterials on their antioxidative and anti-inflammatory activities remains unclear. Moreover, the application of CDs in treating ocular inflammatory diseases remains sparsely documented, indicating an area ripe for further exploration.

By harnessing the neuroprotective properties of curcumin in a nanostructured form, this study not only addresses the limitations of natural curcumin's poor solubility and bioavailability but also leverages the unique biocompatible and highly soluble nature of CQDs prepared from curcumin (Cur) through mild pyrolysis for treating retinal IR injury. This study meticulously demonstrates how Cur-CQDs, particularly those synthesized at 150 °C, significantly mitigate apoptotic cell death, inflammation, and oxidative stress in retinal tissues, as evidenced by marked reductions in TUNEL-positive cell counts and suppressed inflammatory cytokine expression in treated samples. This effect is achieved by modulating key cellular pathways involved in oxidative stress, apoptosis, and inflammation, through the upregulation of antioxidant enzymes and the downregulation of pro-inflammatory cytokines, driven primarily by surface moieties such as cinnamic acid, guaiacol, and ferulic acid. Detailed analysis shows that these nanostructured dots enhance cellular resilience by stabilizing mitochondrial function and reducing cellular permeability changes during ischemic episodes. The findings underscore Cur-CQDs' potential to serve as a novel therapeutic strategy for retinal ischemic conditions, showcasing a significant advancement in ocular neuroprotection research and potential clinical applications. Their profound impact on reducing the pathological features associated with IR injury highlights the transformative potential of nanomedicine in ocular therapeutics.

Experimental section

Cell viability assays

RGC-5 cell line (ATCC, Manassas, VA, US) were maintained in Dulbecco's modified Eagle's medium (DMEM) supplemented with 10% fetal bovine serum (FBS), antibiotic–antimycotic (1%), L-glutamine (2 mM) and nonessential amino acids (1%) in 5% CO_2 at 37 °C. Cells treated with different concentrations of curcumin, Cur-CQDs (see detail on the preparation of Cur-CQDs in ESI†) were then subjected to 6 cycles of intermittent ischemia (each cycle consisted of 0.1% O_2 for 35 minutes and 21% O_2 for 25 minutes) then returned back to normal oxygen concentration for following 18 h. Cell viability was assayed with the use of Cell Counting Kit-8 (CCK-8; Merck) 10 μl per well in dark room avoiding light for 2 h, the absorbance at 450 nm was measured using a microplate reader.

In vivo studies

All animal experiments were performed in compliance with the relevant laws and institutional guidelines, the animal study protocol was approved by the Institutional Animal Care and Use Committee of Chang Gung Memorial Hospital (Approval number: 2020093001; date of approval: 30 September 2020). Four to Five-week-old Sprague–Dawley male albino rats weighing 140–160 g were housed in a temperature-controlled room with a 12-hour light–dark cycle and with free access to food and water. All animals were treated in accordance with the Statement of the Association for Research in Vision and Ophthalmology for Use of Animals in Ophthalmic and Vision Research. Mice were anesthetized with intraperitoneal injections of Zoletil 20 mg kg^{-1} (Virbac, Neurologia, France) mixed with Rompum 10 mg kg^{-1} (Xylazine, Bedford Laboratories, Bedford, OH, USA) and the pupils were dilated with phenylephrine hydrochloride and tropicamide. Intravitreal injection of either Cur-CQDs-150 (100 mg mL^{-1}), curcumin (100 mg mL^{-1}), or phosphate-buffered saline (PBS) was performed in right eye in each rat 3 days before IR injury, left eyes were left untreated. The anterior chamber of the right eye was cannulated with a 27-gauge infusion needle connected to a physiological saline reservoir. The intraocular pressure was increased to 130 mm Hg for 60 minutes

 This journal is © The Royal Society of Chemistry 2025

Published on 05 March 2025. Downloaded by CHANG GUNG UNIVERSITY on 3/26/2025 1:38:55 PM.

by elevating the saline reservoir. Successful achievement of retinal ischemia was confirmed by the collapse of the central retinal artery, and the whitening of the iris during the rise of intraocular pressure.

Immunofluorescence staining

At 24 h after IR injury, immunofluorescence was performed to examine the localization of the hypoxia-induced factor (HIF)-α, the cluster of differentiation (CD) 68 molecule, B-cell lymphoma (BCL)-2, and glucose regulatory protein (Grp) 78. Briefly, rats were euthanized 24 h after IR injury, the eyeballs were embedded in paraffin or Optimal Cutting Temperature (OCT) compound. The tissue specimens were then incubated with one of the following primary antibodies: rabbit polyclonal antibody against rat HIF-α (1:50, Bioss, US), mouse polyclonal antibody against rat CD68 (1:1000, Abcam, Cambridge, UK), mouse monoclonal antibody against rat BCL-2 subunit protein (1:50, Santa Cruz, US), and mouse monoclonal antibody against rat glucose-related protein (Grp78, 1:100, Proteintech, Germany). Immunoreactivity was detected by a fluorescein isothiocyanate (FITC)-labeled or rhodamine-labeled secondary antibody (1:200, Abcam, Cambridge, U.K.), cell nuclei were counterstained with 4′-6-diamidino-2-phenylindole (DAPI).

Western blot analysis

Twenty-four hours following IR injury, rats were euthanized in a CO_2-saturated chamber, anterior segments were removed, and retina wholemounts were isolated and shock frozen at −80 °C within 2 minutes after enucleation. Retinas were later ultrasonically homogenized into 300 μL of a RIPA buffer containing 50 mM Tris (pH 7.4), 150 mM NaCl, 10 mM EDTA, 0.1% SDS, 1% NP-40, 0.5% sodium deoxycholate, 1 mM Na_3VO_4, 1 mM NaF, 1 mM EGTA, 1 mM PMSF and proteinase inhibitor at 4 °C. The protein extracts (20 μg of protein in each lane) were separated by 12% sodium dodecyl sulfate-polyacrylamide gel electrophoresis (SDS-PAGE) and the proteins were transferred to a nitrocellulose membrane. The membranes were then blocked and probed with rabbit polyclonal anti-heme oxygenase (HO)-1 (Abcam, Cambridge, U.K.), anti-GRP78 (Proteintech), anti-CCAAT (C)/enhancer binding protein (EBP)-homologous protein (CHOP) (Santa Cruz), anti-caspase 3 (Abcam), anti-nuclear factor erythroid 2-related factor (Nrf) 2 (Thermo Fisher Scientific) and anti-GAPDH (Santa Cruz) antibody at different dilution. A peroxidase-conjugated anti-rabbit secondary antibody (Perkin-Elmer, USA) was used at a dilution of 1:15000.

Electroretinography (ERG) recordings

The single bright flash electroretinography (ERG) (Retiport, Roland Consult, Germany) under a dark-adapted environment was performed to assess the retinal function of tigecycline-injected eyes and BSS-injected eyes. One or four weeks after intravitreal injection of Cur-CQDs, rats were anesthetized with a solution of ketamine (95 mg mL^{-1}) and xylazine (5 mg mL^{-1}) under dim red light and were kept on a warm pad throughout the procedure. The rats also spent at least 3-hour in dark adaptation before the ERG test. The pupils were then dilated with drops of 0.5% tropicamide. A drop of 0.5% proparacaine hydrochloride was applied for corneal anesthesia; the gold coil-wire electrode was placed on the cornea with 2.5% methylcellulose gel to facilitate the electrode attachment and conduction. The reference and ground electrodes were attached to the forehead and tongue, respectively. The dark-adapted scotopic mixed b-wave response was recorded for measurement of retinal function in each rat. After reducing the background noise to less than 10 Hertz (Hz), a single white flash LED light was used as the standard light stimulus (standard flash: 3 cd s m^{-2}). The 1000-ms interflash interval was determined to be of sufficient duration to prevent carryover effects of successive flashes on the ERG waveform. Responses were amplified with a gain setting ±500 μV and filtered with a bandpass filter (0.3–500 Hz). The overall curve was recorded as the average of 20 collected single responses after removing interference.

Please refer to the provided sections for detailed information on the preparation of Cur-CQDs, the analysis of their antioxidant capacity, *in situ* TUNEL labeling, immunofluorescence staining, and western blot analysis.

Statistical analysis

Data are presented as mean SE. On way analysis of variance (ANOVA) was conducted for comparison. $P < 0.05$ was considered significant.

Results and discussions

Identification of specific moieties on the CQDs

Pyrolyzing curcumin between 120 °C and 180 °C for 2 h yields brownish-orange residues. These residues are further processed in an alkaline medium (200 mM sodium phosphate buffer at pH 12.0), leading to the formation of CQDs.[34–36] The formation of CQDs primarily involves dehydration, polymerization, condensation, and mild carbonization processes (Fig. 1(A)). Initially, the dehydration-induced condensation of curcumin results in the formation of microscale supramolecular structures through polymer cross-linking. Prolonged heating leads to the fragmentation of these structures and further carbonization into spherical Cur-CQDs. The synthesized CQDs, denoted as Cur-CQDs-120, Cur-CQDs-150, and Cur-CQDs-180, correspond to the temperatures (120, 150, and 180 °C, respectively) at which they were prepared. The yield for all Cur-CQDs variants was observed to exceed 90%. Transmission electron microscopy (TEM) analysis reveals a consistent size distribution for all Cur-CQDs, with an average diameter of approximately 4.5 nm (Fig. 1(B)). Dynamic light scattering (DLS) measurements indicate that the hydrodynamic diameters of the Cur-CQDs are around 10 nm, significantly larger than their core sizes measured by TEM. This discrepancy suggests the presence of pyrolytic curcumin polymers encasing the Cur-CQDs surfaces. High-resolution TEM (HR-TEM) images showcase highly crystalline sp^2-hybridized carbon cores with a 0.21 nm interlayer spacing, characteristic of the graphitic carbon (100) plane.[37] Unlike the hydrophobic and water-insoluble curcumin (<1.0 μg mL^{-1}), Cur-CQDs demonstrate remarkable water solubility (>20 mg mL^{-1}) at room

Published on 05 March 2025. Downloaded by CHANG GUNG UNIVERSITY on 3/26/2025 1:38:55 PM.

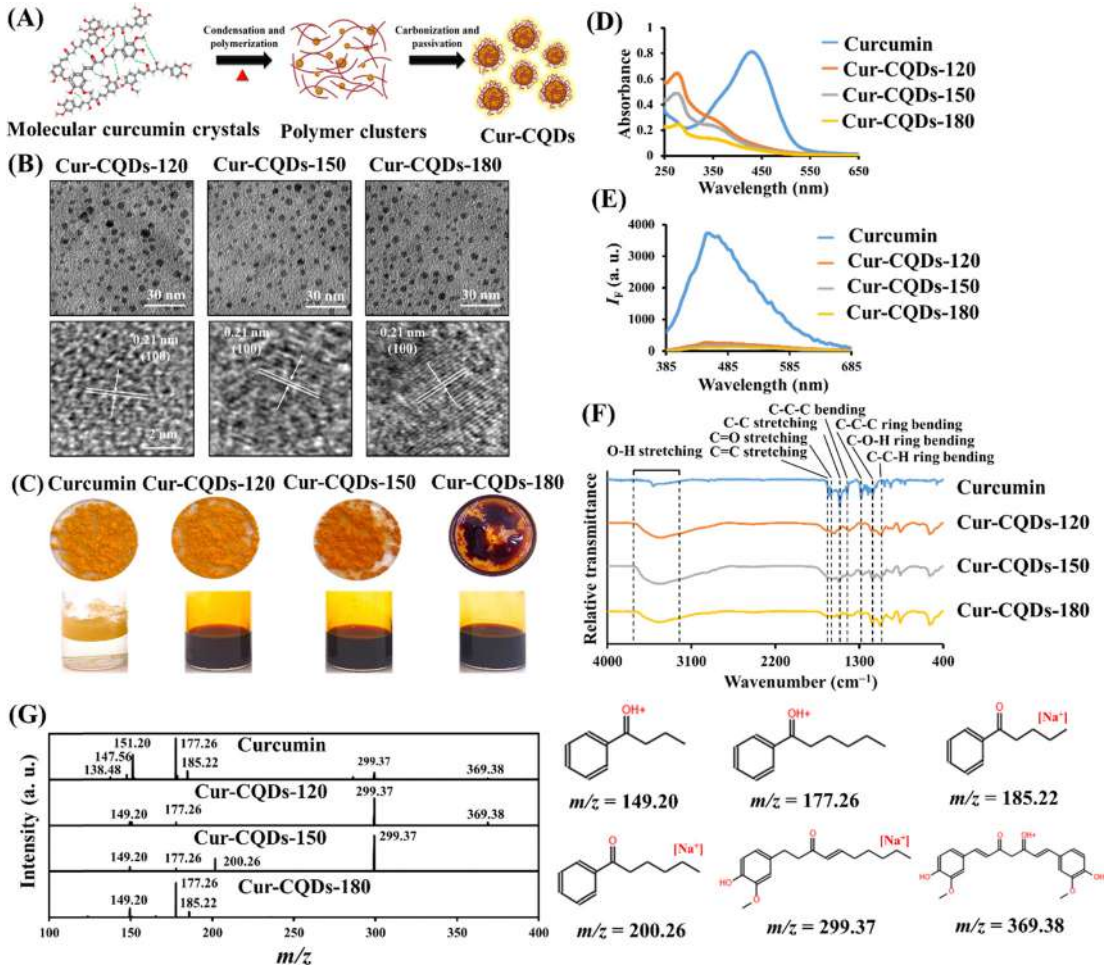


Fig. 1 (A) Schematic representation of the preparation and formation mechanism of Cur-CQDs *via* mild pyrolysis. (B) TEM and HR-TEM images of as-prepared Cur-CQDs. (C) Photographs of curcumin powder and Cur-CQDs (120–180 °C) powder (top panel) and their corresponding aqueous solutions (low panel). (D) UV-Vis absorption and (E) fluorescence spectra of curcumin and Cur-CQDs. The concentration of curcumin or Cur-CQDs was 10 μg mL^{-1}. (F) FTIR and (G) LDI-MS spectra of curcumin and Cur-CQDs.

temperature (Fig. 1(C)). This enhanced solubility, evidenced by a high zeta potential (> −30 mV), is attributed to the dense presence of phenolic and carboxylic groups on the Cur-CQDs surfaces, potentially improving their bioavailability both *in vitro* and *in vivo*. Elemental analysis (EA) indicates a higher oxygen content in Cur-CQDs (>35%) compared to the original curcumin molecule (25%), suggesting the introduction of additional oxygen-containing functional groups during the mild pyrolysis process.

Curcumin exhibits a broad absorption band at 465 nm in the UV-Vis absorption spectrum, indicative of charge-transfer processes within its lowest energy transition (Fig. 1(D)).[38] Conversely, Cur-CQDs display a distinctive peak at 275 nm and a broad shoulder from 310 to 375 nm in their spectra, attributed to $\pi \rightarrow \pi^*$ and $n \rightarrow \pi^*$ transitions, respectively.[36] This highlights the presence of enriched oxygen-containing groups within the CQDs. Under 365 nm excitation, Cur-CQDs emit a very broad fluorescence spectrum, ranging from 400 nm to 600 nm with a low quantum yield (<1%), due to the presence of various-sized polycyclic aromatic or graphene clusters and surface defects (Fig. 1(E)).[39,40] Fourier-transform infrared (FTIR) spectroscopy of Cur-CQDs reveals vibrational signatures similar to those of curcumin (Fig. 1(F)). Lastly, laser desorption/ionization mass spectrometry (LDI-MS) analysis confirms the attachment of numerous curcumin moieties to the Cur-CQDs (Fig. 1(G)). We propose that the fragments observed at various *m*/*z* values represent the diverse moieties such as cinnamic acid-, anisole-, guaiacol, and ferulic acid-like structures on the Cur-CQDs surface, contributing to their anti-inflammatory and neuroprotective activities.[41–46] Cinnamic acid ((2*E*)-3-phenylprop-2-enoic acid) has been extensively studied for its anti-inflammatory properties. It inhibits key enzymes involved in inflammation, such as cyclooxygenase and lipoxygenase, which are crucial in the production of pro-inflammatory mediators.[41] Cinnamic acid derivatives are also explored for their potential neuroprotective effects, possibly through mechanisms involving antioxidative properties and modulation of neuronal pathways.[42] The derivatives of anisole (methoxybenzene) have also shown antioxidative and anti-inflammatory activities.[43] These effects are primarily attributed to their ability to scavenge free

 This journal is © The Royal Society of Chemistry 2025

Published on 05 March 2025. Downloaded by CHANG GUNG UNIVERSITY on 3/26/2025 1:38:55 PM.

radicals and inhibit oxidative stress, which is a common pathway in inflammatory and neurodegenerative diseases. The guaiacol (2-methoxyphenol) also exhibits anti-inflammatory effects by inhibiting enzymes like nitric oxide synthase and cyclooxygenase and modulating other inflammatory pathways.[44,45] Guaiacol and its derivatives also exhibit neuroprotective effects, primarily through their antioxidant mechanisms.[45,46] They upregulate anti-apoptotic proteins, such as B-cell lymphoma 2 (BCL-2), and downregulate pro-apoptotic factors, including caspase-3.[45] Additionally, these compounds modulate signaling pathways involved in cellular survival and stress responses, such as heme oxygenase-1 (HO-1).[46] Also, ferulic acid [(2*E*)-3-(4-hydroxy-3-methoxyphenyl)prop-2-enoic acid] exerts neuroprotective effects on the retina by enhancing cellular antioxidant defenses, such as activating the Nrf2 pathway, which leads to the upregulation of detoxifying enzymes and reduction of oxidative stress.[47] Concurrently, it modulates inflammatory responses through the inhibition of NF-κB signaling, thereby preventing cytokine release and reducing neuronal apoptosis in retinal degenerative conditions.[47]

Cur-CQDs possess minimal toxicity and superior antioxidative activities

Before evaluating bioactivity, we assessed the stability of Cur-CQDs-150 under different environmental conditions by monitoring relative fluorescence changes. As shown in Fig. S1A and B (ESI†), the fluorescence intensity of Cur-CQDs-150 remained stable after incubation in aqueous solution at temperatures up to 95 °C and NaCl concentrations up to 1000 mM, indicating high thermal and salt stability. Additionally, no visible aggregation was observed under these conditions. However, Cur-CQDs-150 exhibited reduced fluorescence and gradual sedimentation in solutions with pH < 6 (Fig. S1C, ESI†), likely due to decreased surface charges and increased hydrogen bonding between CQDs. Furthermore, we investigated the effect of various metal ions (100 μM) on Cur-CQDs-150 fluorescence. Among the tested ions, only mercury (Hg^{2+}) induced significant fluorescence quenching (Fig. S1D, ESI†), primarily due to Hg^{2+}-mediated aggregation, electron transfer, and electron delocalization.[48] These findings highlight the excellent stability of Cur-CQDs-150 in physiological conditions.

Curcumin is widely known for its antioxidative and anti-inflammatory properties.[13,49] Its antioxidative activity is attributed to its ability to scavenge free radicals and enhance the activity of antioxidant enzymes, thus protecting cells from oxidative stress-induced damage.[49] Despite its promising protective effects, the high cytotoxicities of curcumin towards some mammalian cells through inhibiting cell proliferation, triggering apoptosis, and programmed cell death have been reported.[50–52] Therefore, we first assess the antioxidative and cytotoxic effects of Cur-CQDs on cells in comparison to curcumin in its original state. The total antioxidant capacity (TAC) assay based on copper(II) redox reactions is used to measure the antioxidant capacity of vitamins (Vit), curcumin, and Cur-CQDs. Remarkably, Cur-CQDs-150 demonstrated superior antioxidant effectiveness compared to both Vit C and E, which are predominant antioxidants in human eyes,[53] and even surpassed that of free curcumin (Fig. S2A, ESI†). The enhanced antioxidative activity of Cur-CQDs is attributed primarily to their graphitic core structures with multiphenol-like groups on the surfaces, which facilitate rapid electron transfer and hydrogen donation.[54] Additionally, the catalytic carbonyl groups on the edges of the graphitic cores also contribute significantly to these antioxidant properties.[55]

For cytotoxic assays, we exposed retinal ganglion cells (RGC)-5 to varying concentrations of curcumin or Cur-CQDs for 48 h and then assessed cell viability using an MTT assay. RGC-5 are a cell line originally thought to be derived from rat retinal ganglion, which are crucial for transmitting visual information from the eye to the brain. Findings indicated that curcumin adversely affected the viability of RGC-5, reducing survival rates to below 20% even at minimal concentrations of 10 μg mL^{-1} (Fig. S2B, ESI†). Conversely, RGC-5 treated with Cur-CQDs maintained over 80% viability at concentrations up to 100 μg mL^{-1}, showcasing Cur-CQDs' superior biocompatibility. Remarkably, the cytotoxicity threshold of Cur-CQDs was found to be at least 100 times higher than that of curcumin. Curcumin induces cell apoptosis by upregulating pro-apoptotic proteins and downregulating anti-apoptotic proteins, leading to mitochondrial dysfunction and activation of caspase pathways, which trigger the programmed cell death process.[56,57] To investigate whether Cur-CQDs also contribute to suppressing the H_2O_2-induced production of ROS, we utilized a 2′-7′-dichlorodihydrofluorescein diacetate (H_2DCFDA) assay. The results indicated that the generated ROS in the presence of Cur-CQDs is at least five times less ROS than that of curcumin (Fig. S1C, ESI†), corroborating their antioxidative capabilities as observed in the TAC assay. Furthermore, the higher cellular uptake of Cur-CQDs enhances their ability to mitigate oxidative damage within the cells, significantly reducing intracellular ROS levels and contributing to their potent antioxidant effects observed *in vitro*. Cur-CQDs exhibit enhanced cellular uptake due to their smaller size and amphiphilic surface characteristics, which facilitate their entry into cells and increase their interaction with cellular components. Chelating extracellular metal ions by Cur-CQDs would contribute to reducing oxidative stress by limiting the availability of metals that catalyze the formation of ROS.

Superior neuroprotective effects of Cur-CQDs against hypoxia-induced apoptosis

To evaluate the neuroprotective capabilities of different Cur-CQDs, RGC-5 were exposed to curcumin or various Cur-CQDs followed by a 6-h hypoxic insult. This experimental setup involves subjecting RGC-5 to six cycles of hypoxia followed by normoxia (Fig. 2(A)). Each cycle consists of a 35-min exposure to a hypoxic environment with 0.1% O_2, followed by a 25-min return to normoxic conditions with 21% O_2. After these intermittent ischemia cycles, the cells are maintained in normal culture conditions (normoxia) in the presence of curcumin or Cur-CQDs for 18 h. This process, designed to simulate the cellular stress experienced during transient retinal ischemic events, can significantly affect cell viability, mimicking conditions seen in eye diseases such as diabetic retinopathy (DR), retinal vein occlusion (RVO), age-related macular degeneration

Published on 05 March 2025. Downloaded by CHANG GUNG UNIVERSITY on 3/26/2025 1:38:55 PM.

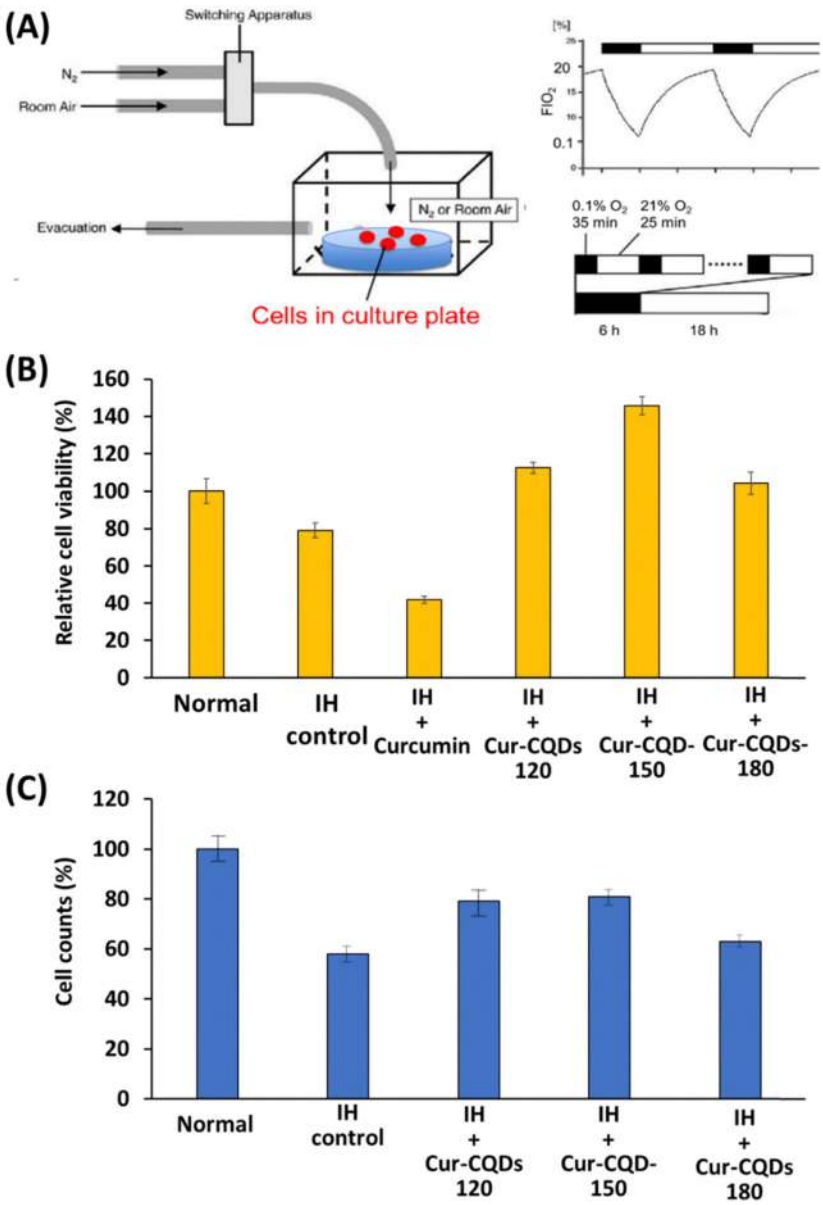


Fig. 2 Neuroprotective effects of Cur-CQDs on retinal cells subjected to hypoxia. (A) Schematic representation of intermittent hypoxia (IH) experiments. (B) Relative cell viability and (C) cell count ratios following exposure to 6 h of IH and 18 h of normoxia. Cells were treated with either curcumin or Cur-CQDs at a concentration of 25 μg mL^{-1}. Data represent the mean ± standard deviation from four independent experiments.

(AMD), central retinal artery occlusion (CRAO), and ischemic optic neuropathy (ION) where fluctuating oxygen levels play a role in disease progression.[58,59] Our results reveal the cells treated with Cur-CQDs-150 at a concentration of 25 μg mL^{-1} demonstrated significantly enhanced viability post-hypoxia compared to those treated with curcumin or other Cur-CQDs (Fig. 2(B)). Specifically, untreated cells showed a survival rate of 58% in the cell counting assay (Fig. 2(C)), whereas treatment with Cur-CQDs-150 resulted in survival rates of 82%. Cur-CQDs-180 treatment resulted in a survival rate of only 65%. Among the tested variants, Cur-CQDs-150 exhibited the most substantial protection against hypoxia-induced cell damage, surpassing both the alternative Cur-CQD formulations and traditional curcumin treatments. This underscores the potential of Cur-CQDs-150 as a formidable candidate for neuroprotective applications in retinal therapies, significantly enhancing cell viability and survival under ischemic conditions.

The LDI-MS analysis reveals distinct surface moieties on Cur-CQDs-150 compared to Cur-CQDs-120 and Cur-CQDs-180 (Fig. 1(G)). The MS spectrum for Cur-CQDs-120 shows intact curcumin molecules (*m*/*z* 369.38), suggesting that some curcumin remained unpyrolyzed and adsorbed onto the CQDs at lower pyrolysis temperatures. Prominent peaks at *m*/*z* 220.26 and 299.37 in Cur-CQDs-150 indicate the presence of abundant cinnamic acid and ferulic acid-based structures. In contrast, Cur-CQDs-180 lacks highly antioxidative guaiacol- and ferulic

 This journal is © The Royal Society of Chemistry 2025

Published on 05 March 2025. Downloaded by CHANG GUNG UNIVERSITY on 3/26/2025 1:38:55 PM.

acid-like moieties, likely due to greater carbonization at higher pyrolysis temperatures. Cur-CQDs-150 excels over other formulations primarily because of its optimal size and surface properties, which facilitate deeper penetration and better retention within cellular structures, thus enhancing its efficacy under hypoxic conditions. The specific *in situ* surface modifications during the mild pyrolysis process of Cur-CQDs-150 likely lead to more effective scavenging of ROS and efficient chelation of metal ions, crucial for mitigating oxidative stress that can cause cell death during ischemic events. Additionally, Cur-CQDs-150 may more effectively modulate cellular pathways, potentially by upregulating anti-apoptotic proteins and downregulating pro-apoptotic signals, providing superior protection against the cellular stress induced by intermittent hypoxia. These unique characteristics position Cur-CQDs-150 as a particularly potent agent for reducing apoptosis typically resulting from ischemic and hypoxic conditions prevalent in various progressive eye diseases.

Evaluation of Cur-CQDs in a rat model of retinal ischemia-reperfusion injury

Curcumin's potential to mitigate hypoxia-induced damage in retinal cells has been well-documented, primarily due to its robust antioxidant and anti-inflammatory properties.[13,49] These properties are critical in combating the oxidative stress and inflammation associated with hypoxic conditions within the retina. Such conditions are notably prevalent in DR and retinal RVO, where they can cause significant tissue damage and consequent vision loss. Our studies extend these findings by demonstrating that Cur-CQDs-150 matches and exceeds curcumin's antioxidative and biocompatibility profiles, adding enhanced protection against hypoxic damage.

Prior to assessing the *in vivo* therapeutic effects of Cur-CQDs, we investigated their ability to penetrate ocular tissues following intravitreal injection. Three days post-injection of Cy5.5-labeled Cur-CQDs, fluorescent signals were observed in various retinal layers, including the RGC layer (RGCL), inner plexiform layer (IPL), inner nuclear layer (INL), and photoreceptors (PR). Remarkably, these signals remained detectable up to 28 days after injection (Fig. S3, ESI†), indicating sustained presence. In contrast, no fluorescent signals were observed in retinas treated with a PBS control. This prolonged retention can be attributed to the small size of Cur-CQDs (<5 nm) and their amphiphilic nature, which confers a high affinity for retinal tissues. The amphiphilic characteristics likely facilitate the Cur-CQDs' integration into the retinal architecture, enhancing their stability and therapeutic efficacy over extended periods. These findings suggest that Cur-CQDs are not only effective in penetrating the retinal barrier but also in sustaining their therapeutic potential within the ocular environment, making them promising candidates for long-term treatments of retinal diseases characterized by hypoxia-related stress.

To evaluate the biocompatibility of Cur-CQDs, we performed flash electroretinography (ERG) at 7 and 28 days post-intravitreal injection. Flash ERG is a sophisticated diagnostic tool used to measure the electrical responses of various cell types within the retina, following exposure to brief flashes of light.[60] This technique is instrumental in determining the potential retinal toxicity of treatments by recording functional changes that might occur after administration. In this study, ERG was employed to assess the ocular biocompatibility of Cur-CQDs treatment in a live subject model, providing insights into the safety and efficacy of the intervention on retinal function. In ERG, the a-wave represents the initial negative response reflecting the photoreceptor activity, primarily from rods and cones, which is crucial for understanding the primary reaction of the retina to light.[60] The b-wave follows the a-wave as a positive peak, originating from the inner retinal cells, primarily bipolar and Müller cells, indicating the secondary response to the visual stimulus.

The ERG results showed no significant differences in the latency or amplitude of the a- and b-waves between the Cur-CQDs-treated left eyes and the PBS-treated right eyes (Fig. 3(A)). Specifically, 7 days after intravitreal injection, the latency of the a-wave was 19.60 ± 1.03 ms in PBS-treated eyes compared to 21.20 ± 0.86 ms in Cur-CQDs-treated eyes ($p > 0.73$; $n = 5$). The amplitude was similarly unaffected, with PBS eyes recording 216.60 ± 15.79 μV and Cur-CQDs eyes 211.40 ± 32.83 μV ($p > 0.18$; $n = 5$). The b-wave latency and amplitude results were also comparable, showing no statistical difference ($p > 0.67$; $n = 5$). Furthermore, the 28 days post-intravitreal injection, the latency of the a-wave remained consistent with earlier observations, at 22.00 ± 2.28 ms for PBS and 22.80 ± 2.04 ms for Cur-CQDs ($P > 0.83$; $n = 5$). The amplitude of the a-wave was 190.40 ± 32.25 μV for PBS and 189.40 ± 19.53 μV for Cur-CQD ($p = 0.900$, $n = 5$). The b-wave metrics followed this trend, demonstrating stable retinal function over time with no significant changes induced by Cur-CQDs treatment. These findings indicate that Cur-CQDs do not adversely affect retinal electrical activity, affirming their safety for potential therapeutic use.

Furthermore, a well-established rat model of retinal ischemia-reperfusion (IR) injury was employed to assess the therapeutic efficacy of Cur-CQDs. The IR injury model, widely recognized for its relevance to human ocular diseases such as acute glaucoma and retinal artery occlusion, involves a temporary occlusion of the central retinal artery.[61] This occlusion provokes an ischemic phase characterized by deprivation of oxygen and nutrients, leading to cellular stress and eventual severe tissue damage. The subsequent reperfusion phase introduces a rapid restoration of blood flow, triggering oxidative stress and inflammatory responses due to the sudden influx of blood components.

Photoreceptors and RGCs, essential for phototransduction and signal transport, are particularly vulnerable due to their high oxygen and energy requirements and dense mitochondrial content.[62] Normally, these mitochondria produce low levels of ROS as byproducts of metabolism. However, ischemic conditions drive a shift from aerobic to anaerobic metabolism, disrupting ion transport across mitochondrial membranes and leading to an excessive accumulation of ROS.[62] This imbalance between ROS and the ocular antioxidant defenses, including vitamins A, C, E, superoxide dismutase (SOD),

Published on 05 March 2025. Downloaded by CHANG GUNG UNIVERSITY on 3/26/2025 1:38:55 PM.

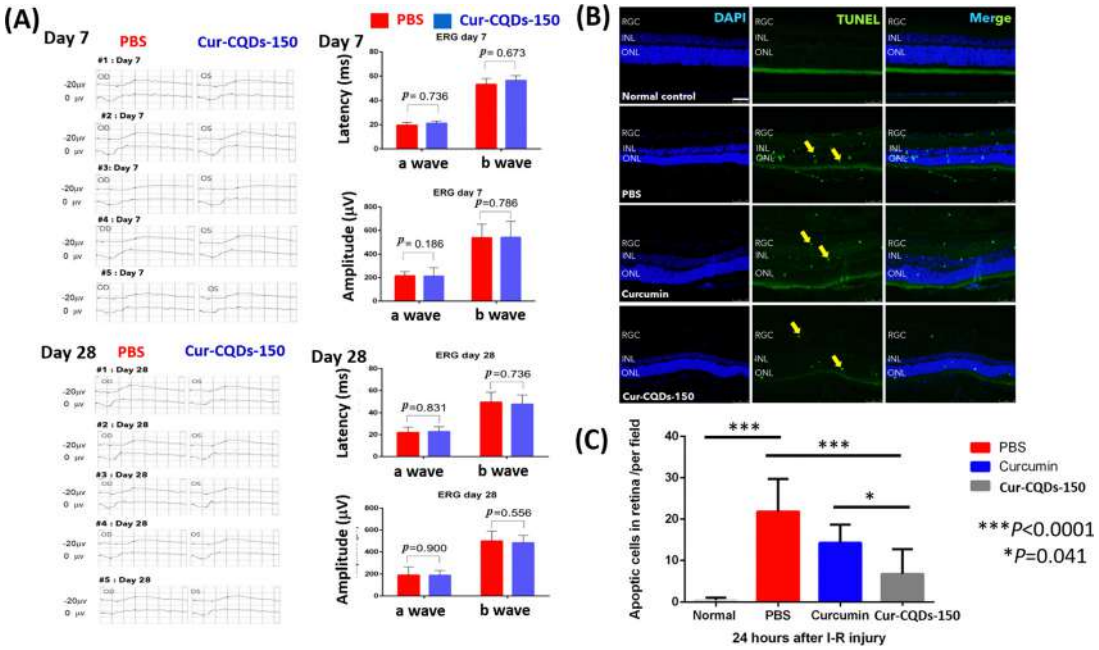


Fig. 3 *In vivo* biocompatibility evaluation of Cur-CQDs and the protective effects of Cur-CQDs-150 on retinal tissues following ischemia-reperfusion (IR) injury. (A) Retinal function assessment *via* flash electroretinography (ERG) following intravitreal injection of Cur-CQDs-150. (B) Apoptosis analysis in retinal tissues 24-h post-IR injury using TUNEL staining. (C) Quantitative evaluation of apoptotic cells across different treatment groups (n = 11). Apoptotic cells (green fluorescence) are indicated by yellow arrows. Scale bar = 500 μm.

glutathione peroxidase, and catalase, defines oxidative stress, which contributes to the heightened susceptibility of the retina and optic nerve to ischemic injury.[63]

In our investigation, the therapeutic impact of Cur-CQDs was quantitatively analyzed *via* TUNEL assays to measure apoptotic cell death (Fig. 3(B) and (C)). Retinas treated with Cur-CQDs-150 demonstrated a significantly lower apoptosis rate (6.8 ± 1.8 cells per field) compared to those treated with PBS (21.8 ± 2.4 cells per field) and curcumin alone (14.3 ± 2.2 cells per field) after 24 h of IR injury. Notably, the apoptosis rate in the Cur-CQDs-150-treated group closely resembled that of healthy retinal tissue [normal (without IR induction); 0.4 ± 0.2 cells per field]. Furthermore, co-labeling with Cy5.5-labeled Cur-CQDs-150 fluorescence and TUNEL staining provided visual confirmation of reduced apoptosis in Cur-CQDs-treated retinas (Fig. S4, ESI†). These findings suggest that the enhanced antioxidative and anti-inflammatory properties of Cur-CQDs substantially mitigate the damage induced by IR events. The superior performance of Cur-CQDs in reducing apoptotic cell counts can be attributed to their potent antioxidative capabilities, which likely interfere with the oxidative stress mechanisms typically activated during reperfusion. Additionally, the anti-inflammatory effects of Cur-CQDs help modulate the inflammatory milieu within the retina, further protecting against cellular damage. Therefore, the application of Cur-CQDs in this model not only underscores their potential in reducing IR-induced retinal injury but also highlights their promise as a novel therapeutic approach for the management of ischemic retinal diseases.

We also conducted hematoxylin and eosin (H&E) staining to evaluate retinal thickness, and the results are presented in Fig. S5 (ESI†) to further assess the therapeutic efficacy of Cur-CQDs-150. Ischemic injury often leads to progressive retinal degeneration, ultimately causing visual impairment. Fig. S5 (ESI†) displays histological images of retinal sections from different test groups, showing a significant loss of RGCs in the PBS-treated group compared to the negative control group (without IR induction), indicating sustained retinal degeneration. Prior to IR injury (negative control group), the retinal thickness was measured at 245 ± 12.4 μm (n = 4) from retinal biopsies. However, after 7 days of IR induction, the retinal thickness decreased to 169.0 ± 22.1 μm and 200.3 ± 6.4 μm in PBS-treated groups (n = 4) and curcumin-treated groups (n = 4), respectively. Notably, the Cur-CQDs-150-treated group maintained a significantly greater retinal thickness 214.3 ± 15.1 μm (n = 4), suggesting enhanced neuroprotection compared to the PBS- and curcumin-treated groups. These findings further demonstrate that Cur-CQDs-150 effectively mitigates ischemic injury, preserving retinal structure and reducing tissue damage.

We further conducted an enzyme-linked immunosorbent assay (ELISA) to quantify IL-1β, IL-18, IL-6, and TNF-α in retinal tissues following IR injury. As shown in Fig. S6 (ESI†), inflammatory cytokine levels were significantly elevated in the PBS-treated group compared to the negative control group (without IR induction), indicating severe inflammation following IR injury. Notably, the Cur-CQDs-150-treated group exhibited significantly lower levels of IL-1β, IL-18, IL-6, and TNF-α compared to the PBS- and curcumin-treated groups, demonstrating the potent anti-inflammatory properties of Cur-CQDs-150. We also quantified malondialdehyde (MDA) levels as an

 This journal is © The Royal Society of Chemistry 2025

Published on 05 March 2025. Downloaded by CHANG GUNG UNIVERSITY on 3/26/2025 1:38:55 PM.

indicator of oxidative stress and evaluated superoxide dismutase (SOD) and glutathione peroxidase (GSH-PX) activities as antioxidant markers in retinal tissues following IR injury. As shown in Fig. S7 (ESI†), MDA levels were significantly elevated in the PBS-treated group compared to the negative control, indicating increased oxidative stress due to IR injury. However, Cur-CQDs-150 treatment significantly reduced MDA levels compared to both PBS- and curcumin-treated groups, demonstrating their ability to suppress oxidative damage. Furthermore, SOD and GSH-PX activities were markedly lower in the PBS-treated group, reflecting compromised antioxidant defenses following IR injury. Notably, Cur-CQDs-150 treatment significantly enhanced both SOD and GSH-PX activities, restoring antioxidant capacity to levels comparable to the negative control. These findings in Fig. S6 and S7 (ESI†) confirm the potent antioxidant and anti-inflammatory properties of Cur-CQDs-150, further supporting their therapeutic potential in mitigating oxidative and inflammatory stress-related retinal damage.

Mechanistic insights into the protective effects of Cur-CQDs on retinal ischemia-reperfusion injury

The protective mechanism of Cur-CQDs-150 against retinal IR injury is primarily attributed to their modulation of key cellular pathways. As depicted in Fig. 4(A), the expression of BCL-2, a critical anti-apoptotic protein, was substantially enhanced in the RGCL of eyes treated with Cur-CQDs-150 compared to those treated with PBS. BCL-2 is a well-known protein to maintain cellular integrity by inhibiting cell death pathways, thereby playing a significant role in the survival of retinal neurons.[64] The elevation in BCL-2 expression, which is more pronounced than in curcumin-treated eyes, underscores the superior ability of Cur-CQDs-150 to inhibit apoptosis pathways and promote neuronal survival under stress conditions.

Furthermore, the anti-inflammatory and anti-hypoxic effects of Cur-CQDs-150 are evident through the minimal expression of CD68 and activation of hypoxia-inducible factor 1α (HIF-1α), as illustrated in Fig. 4(B) and (C). Staining for CD68 in the retina is utilized to detect and quantify the presence of macrophages and activated microglia.[65] This method is pivotal for assessing inflammatory responses within the retinal tissue, helping to elucidate the immune dynamics associated with various ocular diseases and injury recovery processes. The reduced CD68 staining in Cur-CQD-150-treated eyes reflects a diminished macrophage and microglia activation, indicating a lower inflammatory response. This is critical as excessive inflammation can exacerbate neuronal damage during IR events. Similarly, the subdued activation of HIF-1α in Cur-CQDs-150-treated eyes suggests a mitigated cellular response to hypoxia. HIF-1α is a regulatory protein that responds to oxygen deficiency by promoting angiogenesis and altering metabolic pathways to adapt to hypoxic conditions.[66] Its reduced activation in the presence of Cur-CQDs-150 may reflect an environment with less cellular stress and a stabilized oxygen supply, further protecting the retina from the detrimental effects of ischemia.

Additionally, the modulation of endoplasmic reticulum (ER) stress markers highlights another dimension of Cur-CQDs-150's protective mechanisms. Fig. 4(D) shows significant upregulation of glucose-regulated protein 78 (Grp 78), a marker of ER stress,[67] in the IPL of retinas treated with PBS post-ischemic injury. In contrast, the expression of Grp78 is notably reduced in retinas treated with Cur-CQDs-150, suggesting effective mitigation of ER stress. This reduction in Grp 78 expression indicates a broader neuroprotective effect, encompassing the activation of survival proteins like BCL-2, reduction of hypoxic transcriptional proteins such as HIF-α, amelioration of retinal inflammation, and the abolishment of ER stress following ischemic injury. Notably, the immunostaining patterns of BCL-2, CD68, HIF-1α, and Grp78 in Cur-CQDs-150-treated retinas closely match those of healthy retinal tissue (negative control, without IR induction) (Fig. 4(A)–(D)), reinforcing their potential as a therapeutic strategy for ischemic retinal diseases.

Western blot analysis provided further crucial insights into the molecular dynamics within the retina post-IR injury, as shown in Fig. 4(E) and (F). The study highlighted a significant increase in the expression of key stress-related and apoptotic proteins, including Grp 78, nuclear factor erythroid 2-related factor 2 (Nrf2), C/EBP homologous protein (CHOP), caspase 3, and heme oxygenase-1 (HO-1) following IR injury. These proteins are indicative of ER stress and the activation of apoptosis pathways, which contribute to cellular damage under ischemic conditions.[67–71] The levels of Grp 78, Nrf2, CHOP, an caspase 3 were substantially lower in retinas treated with the Cur-CQDs compared to those treated with PBS and curcumin, suggesting a robust protective effect against ER stress and apoptosis. This reduction points to the ability of Cur-CQDs to stabilize retinal cellular environments, curtailing the cascade of cellular destruction triggered by ischemia.

Furthermore, the analysis revealed a more pronounced upregulation of heme HO-1 in the Cur-CQDs treated group. HO-1 is an essential antioxidant protein that plays a pivotal role in cellular defense mechanisms against oxidative stress.[71] Its enhanced expression underlines the antioxidant capacity of Cur-CQDs, which helps in neutralizing the oxidative bursts frequently observed after reperfusion injuries. Interestingly, the expression of Nrf2, a key regulator of antioxidant defense mechanisms,[68] was significantly elevated in the retinas treated with PBS and curcumin post-injury. However, in Cur-CQDs-150 treated eyes, Nrf2 levels were comparatively reduced. This observation suggests that while Nrf2 activation is a response to oxidative stress, Cur-CQDs-150 may reduce the overall oxidative stress level so effectively that the demand for Nrf2 activation is diminished. This indicates not just a reactive antioxidant response but a fundamental enhancement of cellular resilience against oxidative stress. Moreover, the western blot results for Grp78, Nrf2, CHOP, caspase 3, and HO-1 in Cur-CQDs-150-treated retinas closely matched those of the negative control group (without IR induction), further supporting their therapeutic potential for ischemic retinal diseases.

These immunostaining and western blotting findings collectively highlight the dual protective action of Cur-CQDs-150 against both apoptosis and inflammation, crucial for preserving retinal integrity during IR injury. By bolstering

Published on 05 March 2025. Downloaded by CHANG GUNG UNIVERSITY on 3/26/2025 1:38:55 PM.

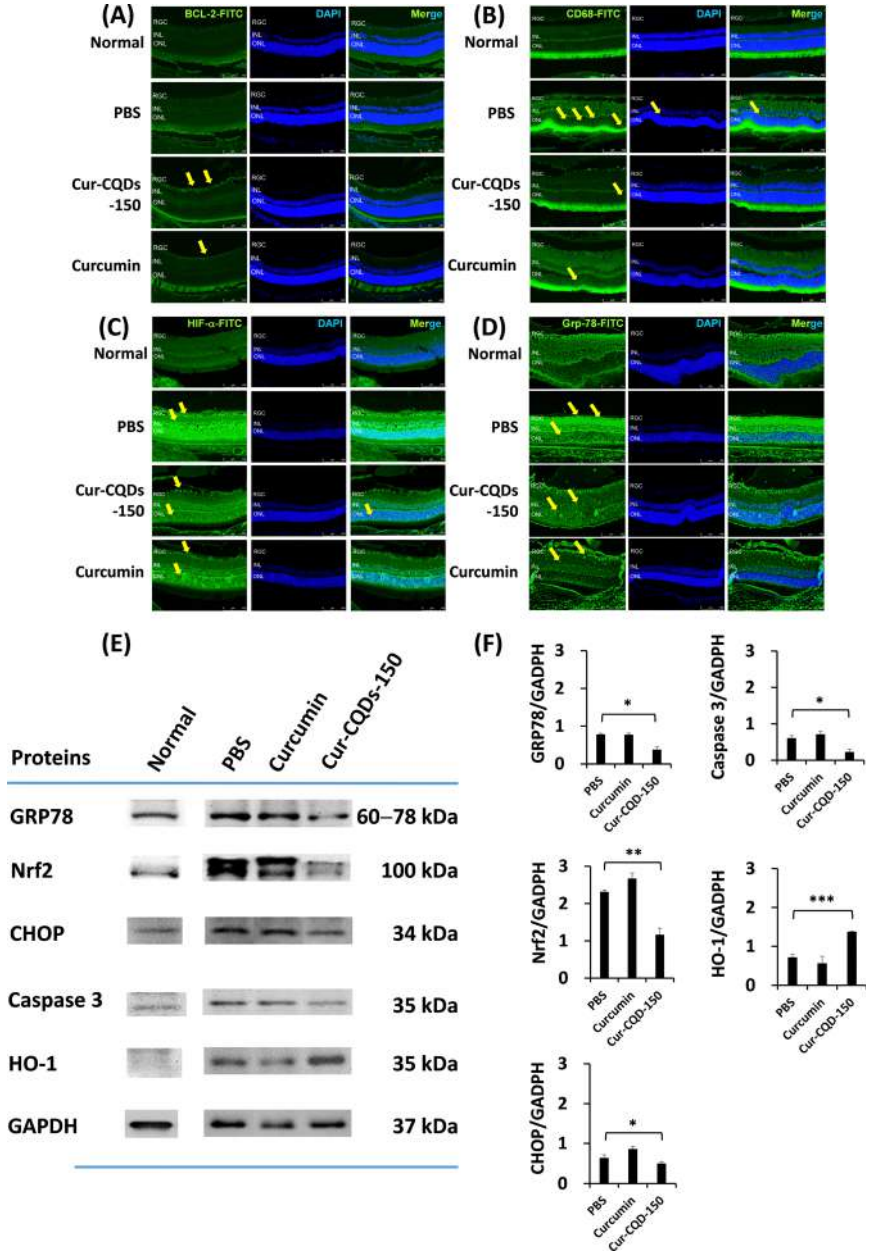


Fig. 4 Immunostaining and western blot analysis after IR injury. (A)–(D) The immunostaining images present immunofluorescence analysis of key proteins including (A) BCL-2, (B) CD68, (C) HIF-1α, and (D) Grp 78 following IR injury. Yellow arrows highlight fluorescent signals (green) of expressed cytokines or proteins. Scale bar = 100 μm. (E), (F) Western blot analysis of protein expression following retinal IR injury. Samples were collected from the retinal tissues of rats subjected to 60 min of ischemia followed by 24 h of reperfusion. The retinas were treated with PBS, curcumin or Cur-CQDs-150 prior to injury induction. Protein lysates were prepared using RIPA buffer, and equal amounts of protein were loaded onto SDS-PAGE gels for separation followed by immunoblotting. *$p < 0.05$, **$p < 0.01$, ***$p < 0.001$.

anti-apoptotic defenses and tempering inflammatory and hypoxic responses, Cur-CQDs-150 showcases potential as a therapeutic agent for managing retinal ischemic conditions, offering insights into potent treatment strategies for ocular diseases characterized by ischemic and hypoxic challenges.

Curcumin is celebrated for its potent antioxidant capabilities, primarily due to its effectiveness in scavenging various ROS such as superoxide anions, hydroxyl radicals, hydrogen peroxide, singlet oxygen, and nitric oxide.[49,72–74] The antioxidant properties of curcumin are defined by its complex molecular structure, which includes multiple functional groups that contribute to its effectiveness. These include phenolic rings, which act as electron traps to reduce hydrogen peroxide formation and scavenge superoxide radicals; the β-diketo group, which is involved in metal–ligand complexation; and carbon–carbon double bonds.[72–74] Together, these structural elements enhance curcumin's capability to counteract oxidative stress. This activity not only protects cells from damage but also facilitates the upregulation of the Nrf2

 This journal is © The Royal Society of Chemistry 2025

Published on 05 March 2025. Downloaded by CHANG GUNG UNIVERSITY on 3/26/2025 1:38:55 PM.

pathway,[75,76] a critical regulator that enhances cellular defense mechanisms against oxidative stress. Despite these benefits, our studies noted that in treatments using Cur-CQDs-150, Nrf2 activation was unexpectedly low, while the expression of the antioxidant protein HO-1 was significantly elevated, suggesting that Cur-CQDs-150 might trigger protective mechanisms in the retina independently of the Nrf2 pathway. Additionally, curcumin's potent anti-inflammatory effects, achieved through the inhibition of pathways such as NF-κB and COX-2, contribute to its neuroprotective actions against retinal ischemia-reperfusion injury by mitigating inflammation, apoptosis, and oxidative stress.[77,78] Despite these benefits, the clinical utility of curcumin is constrained by its poor solubility and bioavailability, leading to the development of various nanoformulations like nanomicelles and nano-encapsulations to enhance its delivery.[79–82] Unlike these complex formulations, the synthesis of Cur-CQDs is relatively straightforward, offering a viable alternative with lower cytotoxicity and enhanced antioxidative and anti-inflammatory activities compared to conventional curcumin treatments.

The simplicity of preparation and promising efficacy of Cur-CQDs position them as potential therapeutic agents for clinical use. However, to fully ascertain their clinical viability and therapeutic potential in treating retinal and other oxidative stress-related diseases, comprehensive studies and advances are necessary. Extensive clinical trials are essential to evaluate the safety and efficacy of Cur-CQDs in humans, including studies on pharmacokinetics, biocompatibility, and potential long-term effects. These trials should also explore various dosing regimens to identify the optimal therapeutic concentration that balances efficacy with minimal side effects. Additionally, the scalability of the synthesis process must be enhanced to ensure that Cur-CQDs can be produced in sufficient quantities under good manufacturing practice (GMP) conditions. Developing targeted delivery systems to direct Cur-CQDs more specifically to diseased tissues could further improve therapeutic outcomes and reduce systemic exposure. Lastly, investigating the mechanistic pathways influenced by Cur-CQDs will be crucial for tailoring these nanoparticles to specific clinical conditions, potentially extending their applications beyond ocular conditions to a broader range of diseases characterized by oxidative stress and inflammation.

Conclusions

Our study on Cur-CQDs highlights a significant advancement in the field of ocular therapeutics, especially in managing retinal IR injury. Cur-CQDs synthesized at 150 °C, which are characterized by their surface moieties of guaiacol and ferulic acid, have shown exceptional capabilities in reducing apoptosis, alleviating inflammation, and bolstering antioxidant defenses within the retinal tissues. The superior performance of Cur-CQDs over traditional curcumin formulations can be attributed to their enhanced bioavailability, lower cytotoxicity, and robust anti-inflammatory and antioxidative activities. These properties make Cur-CQDs a promising candidate for clinical applications in treating ischemic retinal diseases. Moreover, the benefits of Cur-CQDs relative to the CQDs derived from other phytochemicals include their inherent anti-inflammatory properties, high biocompatibility, and effective penetration and integration into retinal tissues for extended durations. These features ensure sustained therapeutic effectiveness and reduced side effects, essential for successfully managing chronic ocular diseases. As the field progresses, further exploration into the mechanistic pathways influenced by Cur-CQDs will be vital in optimizing their therapeutic potential and extending their application to other oxidative stress-related diseases.

Author contributions

Ming-Hui Sun: investigation, conceptualization, methodology, writing – original draft, review & editing, project administration, funding acquisition. Kuan-Jen Chen: data curation, writing – original draft. Yu-Ting Tsao: data curation, Chi-Chin Sun: supervision, Jui-Yang Lai: supervision. Chin-Jung Lin: data curation, writing – original Draft. Yu-Fen Huang: supervision. Chih-Ching Huang: conceptualization, visualization, writing – review & editing, supervision.

Data availability

The data supporting this article have been included as part of the ESI.†

Conflicts of interest

The authors declare that they have no known competing financial interests or personal relationships that could have appeared to influence the work reported in this paper.

Acknowledgements

This research was funded by a research grant from Chang Gung Memorial Hospital (CMRPG3K2271) and the National Science and Technology Council (NSTC 112-2314-B-182A-022, 113-2113-M-019-001, 113-2113-M-019-001, 112-2622-B-019-006).

References

1 A. Zia, T. Farkhondeh, A. M. Pourbagher-Shahri and S. Samarghandian, *Biomed. Pharmacother.*, 2021, **134**, 111119.
2 R. M. F. Bássoli, D. Audi, B. J. Ramalho, M. Audi, K. R. Quesada and S. M. Barbalho, *J. Herb. Med.*, 2023, **42**, 100771.
3 A. B. Kunnumakkara, M. Hegde, D. Parama, S. Girisa, A. Kumar, U. D. Daimary, P. Garodia, S. C. Yenisetti, O. V. Oommen and B. B. Aggarwal, *ACS Pharmacol. Transl. Sci.*, 2023, **6**, 447–518.
4 H.-M. Wang, Y.-X. Zhao, S. Zhang, G.-D. Liu, W.-Y. Kang, H.-D. Tang, J.-Q. Ding and S.-D. Chen, *J. Alzheimer's Dis.*, 2010, **20**, 1189–1199.

Published on 05 March 2025. Downloaded by CHANG GUNG UNIVERSITY on 3/26/2025 1:38:55 PM.

5 J. Trujillo, L. F. Granados-Castro, C. Zazueta, A. C. Anderica-Romero, Y. I. Chirino and J. Pedraza-Chaverri, *Arch. Pharm.*, 2014, **347**, 873–884.
6 H.-J. Zhang, Y.-Q. Xing, W. Jin, D. Li, K. Wu and Y. Lu, *Int. J. Clin. Exp. Pathol.*, 2015, **8**, 9223–9231.
7 S. Wang, Q. Ye, J. Tu, M. Zhang and B. Ji, *Clin. Exp. Hypertens.*, 2017, **39**, 711–717.
8 M. Mohamadian, N. Parsamanesh, H. Chiti, T. Sathyapalan and A. Sahebkar, *Phytother. Res.*, 2022, **36**, 4299–4324.
9 L. Zhang, Y. Han, X. Wu, B. Chen, S. Liu, J. Huang, L. Kong, G. Wang and Z. Ye, *Apoptosis*, 2023, **28**, 1285–1303.
10 Y.-K. Yue, B. Mo, J. Zhao, Y.-J. Yu, L. Liu, C.-L. Yue and W. Liu, *J. Ocul. Pharmacol. Ther.*, 2014, **30**, 657–664.
11 A. Memarzia, M. R. Khazdair, S. Behrouz, Z. Gholamnezhad, M. Jafarnezhad, S. Saadat and M. H. Boskabady, *BioFactors*, 2021, **47**, 311–350.
12 M. Hao, Y. Chu, J. Lei, Z. Yao, P. Wang, Z. Chen, K. Wang, X. Sang, X. Han, L. Wang and G. Cao, *Aging Dis.*, 2023, **14**, 716–749.
13 B. M. Davis, M. Pahlitzsch, L. Guo, S. Balendra, P. Shah, N. Ravindran, G. Malaguarnera, C. Sisa, E. Shamsher, H. Hamze, A. Noor, A. Sornsute, S. Somavarapu and M. F. Cordeiro, *Sci. Rep.*, 2018, **8**, 11066.
14 P. Xiong, X. Huang, N. Ye, Q. Lu, G. Zhang, S. Peng, H. Wang and Y. Liu, *Adv. Sci.*, 2022, **9**, e2106049.
15 G. Sanità, B. Carrese and A. Lamberti, *Front. Mol. Biosci.*, 2020, **25**, 587012.
16 K. S. Jaiswal, O. Malka, N. Shauloff, M. Bersudsky, E. Voronov, B. Gupta and R. Jelinek, *Colloids Surf., B*, 2023, **223**, 113173.
17 Y. Ma, J. Zhao, L. Cheng, C. Li, X. Yan, Z. Deng, Y. Zhang, J. Liang, C. Liu and M. Zhang, *Carbon*, 2023, **204**, 526–537.
18 H. Geng, J. Chen, K. Tu, H. Tuo, Q. Wu, J. Guo, Q. Zhu, Z. Zhang, Y. Zhang, D. Huang, M. Zhang and Q. Xu, *J. Nanobiotechnol.*, 2023, **21**, 500.
19 J. Yu, X. Huang, X. Chen, P. Hu, T. Liu, T. Zhang, R. Cheng, T. Cui and J. Li, *Carbon*, 2024, **226**, 119202.
20 J. Lv, H. Tian, L. Pan, Z. Chen, M. Li, R. A. Ghiladi, Z. Qin and X. Yin, *Chem. Eng. Sci.*, 2024, **295**, 120084.
21 D. Li, K. Y. Xu, W. P. Zhao, M. F. Liu, R. Feng, D. Q. Li, J. Bai and W. L. Du, *Front. Pharmacol.*, 2022, **13**, 815479.
22 A. Sharma, H. K. Choi and H. J. Lee, *Oxid. Med. Cell. Longevity*, 2023, **2023**, 3076119.
23 P. Innocenzi and L. Stagi, *Nano Today*, 2023, **50**, 101837.
24 Y. Li, W. Li, X. Yang, Y. Kang, H. Zhang, Y. Liu and B. Lei, *ACS Appl. Nano Mater.*, 2021, **4**, 113–120.
25 F. Gao, J. Liu, P. Gong, Y. Yang and Y. Jiang, *Chem. Eng. J.*, 2023, **462**, 142338.
26 W. Gao, J. He, L. Chen, X. Meng, Y. Ma, L. Cheng, K. Tu, X. Gao, C. Liu, M. Zhang, K. Fan, D. Pang and X. Yan, *Nat. Commun.*, 2023, **14**, 160.
27 Y. Jin, Q. Zhang, X. Qin, Z. Liu, Z. Li, X. Zhong, L. Xia, J. He and B. Fang, *J. Nanobiotechnol.*, 2022, **20**, 469.
28 R. Qiang, H. Huang, J. Chen, X. Shi, Z. Fan, G. Xu and H. Qiu, *ACS Appl. Mater. Interfaces*, 2023, **15**, 38653–38664.
29 W. Guo, M. Ji, Y. Li, M. Qian, Y. Qin, W. Li, H. Nie, W. Lv, G. Jiang, R. Huang, C. Lin, H. Li and R. Huang, *Biomaterials*, 2024, **309**, 122622.
30 L. Bao, W. Luo, Q. Li, Y. Zhang, Z. Zhang, X. Li, L. Wang, J. Zhang, K. Huang, X. Yu and L. Xu, *Carbon*, 2024, **228**, 119333.
31 S. M. ElMorsy, D. A. Gutierrez, S. Valdez, J. Kumar, R. J. Aguilera, M. Noufal, H. Sarma, S. Chinnam and M. Narayan, *J. Colloid Interface Sci.*, 2024, **670**, 357–363.
32 P. Ye, L. Li, X. Qi, M. Chi, J. Liu and M. Xie, *J. Colloid Interface Sci.*, 2023, **650**, 1749–1761.
33 J. L. Lim, C.-J. Lin, C.-C. Huang and L.-C. Chang, *Colloids Surf., B*, 2024, **234**, 113676.
34 C.-J. Lin, T.-L. Hwang, R. Y. L. Wang, A. Nain, R.-H. Shih, L. Chang, H.-J. Lin, S. G. Harroun, H.-T. Chang and C.-C. Huang, *Small*, 2024, e2307210.
35 H.-H. Chen, C.-J. Lin, A. Anand, H.-J. Lin, H.-Y. Lin, J.-Y. Mao, P.-H. Wang, Y. J. Tseng, W.-S. Tzou and C.-C. Huang, *J. Biol. Chem.*, 2022, **298**, 101957.
36 C.-J. Lin, L. Chang, H.-W. Chu, H.-J. Lin, P.-C. Chang, R. Y. L. Wang, B. Unnikrishnan, J.-Y. Mao, S.-Y. Chen and C.-C. Huang, *Small*, 2019, **15**, e1902641.
37 S. Y. Yang, J.-S. Park, H. Y. Koo, Y. C. Kang and A. Okbaz, *Int. J. Energy Res.*, 2023, 9881400.
38 A. Dutta, B. Boruah, A. K. Manna, B. Gohain, P. M. Saikia and R. K. Dutta, *Spectrochim. Acta, Part A*, 2013, **104**, 150–157.
39 M. Langer, M. Paloncýová, M. Medveď, M. Pykal, D. Nachtigallová, B. Shi, A. J. A. Aquino, H. Lischka and M. Otyepka, *Appl. Mater. Today*, 2021, **22**, 100924.
40 M. Fu, F. Ehrat, Y. Wang, K. Z. Milowska, C. Reckmeier, A. L. Rogach, J. K. Stolarczyk, A. S. Urban and J. Feldmann, *Nano Lett.*, 2015, **15**, 6030–6035.
41 D. Hadjipavlou-Litina and E. Pontiki, *Methods Mol. Biol.*, 2015, **1208**, 361–377.
42 T. Prorok, M. Jana, D. Patel and K. Pahan, *Neurochem. Res.*, 2019, **44**, 751–762.
43 S. K. Murari and M. V. Shwetha, *J. Food Sci. Technol.*, 2016, **53**, 840–847.
44 D.-R. Zhao, Y.-S. Jiang, J.-Y. Sun, H.-H. Li, X.-L. Luo and M.-M. Zhao, *J. Agric. Food Chem.*, 2019, **67**, 1230–1243.
45 T. Esatbeyoglu, K. Ulbrich, C. Rehberg, S. Rohn and G. Rimbach, *Food Funct.*, 2015, **6**, 887–893.
46 W.-T. Weng, P.-C. Kuo, B. A. Scofield, H. C. Paraiso, D. A. Brown, I.-C. Yu and J.-H. Yen, *Front. Immunol.*, 2022, **13**, 887000.
47 Y. Wang, Y. Huo, L. Zhao, F. Lu, O. Wang, X. Yang, B. Ji and F. Zhou, *Mol. Nutr. Food Res.*, 2016, **60**, 1564–1577.
48 D. Dai, C. Zhang, N. T. D. Thuy, G. Zhao, W. Lu and J. Fan, *Diamond Relat. Mater.*, 2022, **126**, 109076.
49 L. Arshad, M. A. Haque, S. N. Abbas Bukhari and I. Jantan, *Future Med. Chem.*, 2017, **9**, 605–626.
50 A. Haverić, S. Haverić, M. Hadžić, N. Lojo-Kadrić and S. Ibrulj, *Cell. Mol. Biol.*, 2018, **64**, 87–91.
51 I. Silva de Sá, A. P. Peron, F. V. Leimann, G. N. Bressan, B. N. Krum, R. Fachinetto, J. Pinela, R. C. Calhelha, M. F. Barreiro, I. Ferreira, O. H. Gonçalves and R. P. Ineu, *Food Chem. Toxicol.*, 2019, **125**, 29–37.
52 M. A. Romero-Hernández, P. Eguía-Aguilar, M. Perézpeña-DiazConti, A. Rodríguez-Leviz, S. Sadowinski-Pine,

 This journal is © The Royal Society of Chemistry 2025

Published on 05 March 2025. Downloaded by CHANG GUNG UNIVERSITY on 3/26/2025 1:38:55 PM.

L. A. Velasco-Rodríguez, J. R. Cáceres-Cortés and F. Arenas-Huertero, *Toxicol. Mech. Methods*, 2013, **23**, 650–659.
53 Y.-J. Hsueh, Y.-N. Chen, Y.-T. Tsao, C.-M. Cheng, W.-C. Wu and H.-C. Chen, *Int. J. Mol. Sci.*, 2022, **23**, 1255.
54 Q. Li, X. Shen and D. Xing, *Dyes Pigm.*, 2023, **208**, 110784.
55 C. Dong, X. Ma, Y. Huang, Y. Zhang and X. Gao, *Front. Bioeng. Biotechnol.*, 2022, **10**, 943399.
56 N. E. Rainey, A. Moustapha and P. X. Petit, *Oxid. Med. Cell. Longevity*, 2020, **2020**, 3656419.
57 N. I. Ismail, I. Othman, F. Abas, H. L. N and R. Naidu, *Int. J. Mol. Sci.*, 2019, **20**, 2454.
58 M. Mentek, J. Morand, M. Baldazza, G. Faury, F. Aptel, J. L. Pepin, D. Godin-Ribuot and C. Chiquet, *Invest. Ophthalmol. Vis. Sci.*, 2018, **59**, 5256–5265.
59 K. D. Beharry, C. L. Cai, P. Sharma, V. Bronshtein, G. B. Valencia, D. R. Lazzaro and J. V. Aranda, *Invest. Ophthalmol. Vis. Sci.*, 2013, **54**, 7644–7657.
60 J. J. McAnany, O. S. Persidina and J. C. Park, *Surv. Ophthalmol.*, 2022, **67**, 712–722.
61 G. Minhas, J. Sharma and N. Khan, *Front. Immunol.*, 2016, **7**, 444.
62 E. Borrelli, F. Bandello, C. J. F. Boon, V. Carelli, G. Lenaers, M. Reibaldi, S. R. Sadda, A. A. Sadun, D. Sarraf, P. Yu-Wai-Man and P. Barboni, *Prog. Retinal Eye Res.*, 2024, **101**, 101264.
63 S.-Y. Li, Z. J. Fu and A. C. Lo, *Oxid. Med. Cell. Longevity*, 2012, **2012**, 426769.
64 T. Lindsten, W. X. Zong and C. B. Thompson, *Neuroscientist*, 2005, **11**, 10–15.
65 M. Choudhary and G. Malek, *Adv. Exp. Med. Biol.*, 2023, **1415**, 207–213.
66 S. Huang, K. Cao, C. Wang, P. Chen, Y. Chen, Y. Zhang, S. Yu, Z. Bai, S. Guo, M. Liao, Q. Li, G. Zhang, J. He and Y. Xu, *Acta Pharmacol. Sin.*, 2024, **45**, 1438–1450.
67 Y. Wang, S. Gao, Y. Zhu and X. Shen, *Curr. Eye Res.*, 2017, **42**, 1202–1208.
68 J. Zhang, T. Zhang, S. Zeng, X. Zhang, F. Zhou, M. C. Gillies and L. Zhu, *Biomedicines*, 2023, **11**, 15122.
69 H. Li, X. Zhu, F. Fang, D. Jiang and L. Tang, *Neurosci. Lett.*, 2014, **575**, 68–73.
70 J. Li, J. Lu, G. Chen and D. Li, *World J. Tradit. Chin. Med.*, 2022, **8**, 241–246.
71 Z. Tang, Y. Ju, X. Dai, N. Ni, Y. Liu, D. Zhang, H. Gao, H. Sun, J. Zhang and P. Gu, *Redox Biol.*, 2021, **43**, 101971.
72 I. G. David, E. E. Iorgulescu, D. E. Popa, M. Buleandra, M. C. Cheregi and H. Noor, *Antioxidants*, 2023, **12**, 1908.
73 N. S. Jha, S. Mishra, S. K. Jha and A. Surolia, *Electrochim. Acta*, 2015, **151**, 574–583.
74 B. Kumar, V. Singh, R. Shankar, K. Kumar and R. K. Rawal, *Curr. Top. Med. Chem.*, 2017, **17**, 148–161.
75 T. Xie, X. Chen, W. Chen, S. Huang, X. Peng, L. Tian, X. Wu and Y. Huang, *Front. Pharmacol.*, 2021, **12**, 796565.
76 H. Meng, J. Wu, L. Shen, G. Chen, L. Jin, M. Yan, H. Wan and Y. He, *Int. J. Biol. Macromol.*, 2022, **215**, 398–412.
77 H. Yang, S. Huang, Y. Wei, S. Cao, C. Pi, T. Feng, J. Liang, L. Zhao and G. Ren, *J. Cancer*, 2017, **8**, 3697–3706.
78 J. Yuan, R. Liu, Y. Ma, Z. Zhang and Z. Xie, *Inflammation*, 2018, **41**, 1804–1814.
79 D. Aggarwal, M. Chaudhary, N. Bajaj, D. Sharma, S. K. Upadhyay, V. K. Garg, H. S. Abdulabbas, H. S. Tuli and I. Rani, *Curr. Bioact. Compd.*, 2024, **20**, 10–20.
80 N. Sabouni, H. Z. Marzouni, S. Palizban, S. Meidaninikjeh, P. Kesharwani, T. Jamialahmadi and A. Sahebkar, *J. Drug Targeting*, 2023, **31**, 243–260.
81 V. S. Ipar, A. Dsouza and P. V. Devarajan, *Eur. J. Drug Metab. Pharmacokinet.*, 2019, **44**, 459–480.
82 M. Gera, N. Sharma, M. Ghosh, D. L. Huynh, S. J. Lee, T. Min, T. Kwon and D. K. Jeong, *Oncotarget*, 2017, **8**, 66680–66698.